

Supporting Information

Efficient Development of Neural Network Potential for Pure Silica Zeolites

Sunday J. Ogenyi,[†] Yusuf Shaidu,[‡] Nicola Seriani,[¶] and Omololu Akin-Ojo^{*,§}

[†]*Condensed Matter Section, East African Institute for Fundamental Research (EAIFR),
University of Rwanda, Kigali, Rwanda*

[‡]*Department of Physics, University of California Berkeley, Berkeley, California 94720,
United States*

[¶]*Condensed Matter Section, The Abdus Salam International Centre for Theoretical Physics
(ICTP), I-34151 Trieste, Italy*

[§]*Condensed Matter Section, Department of Physics, University of Ibadan, Nigeria*

E-mail: oakinojo@gmail.com

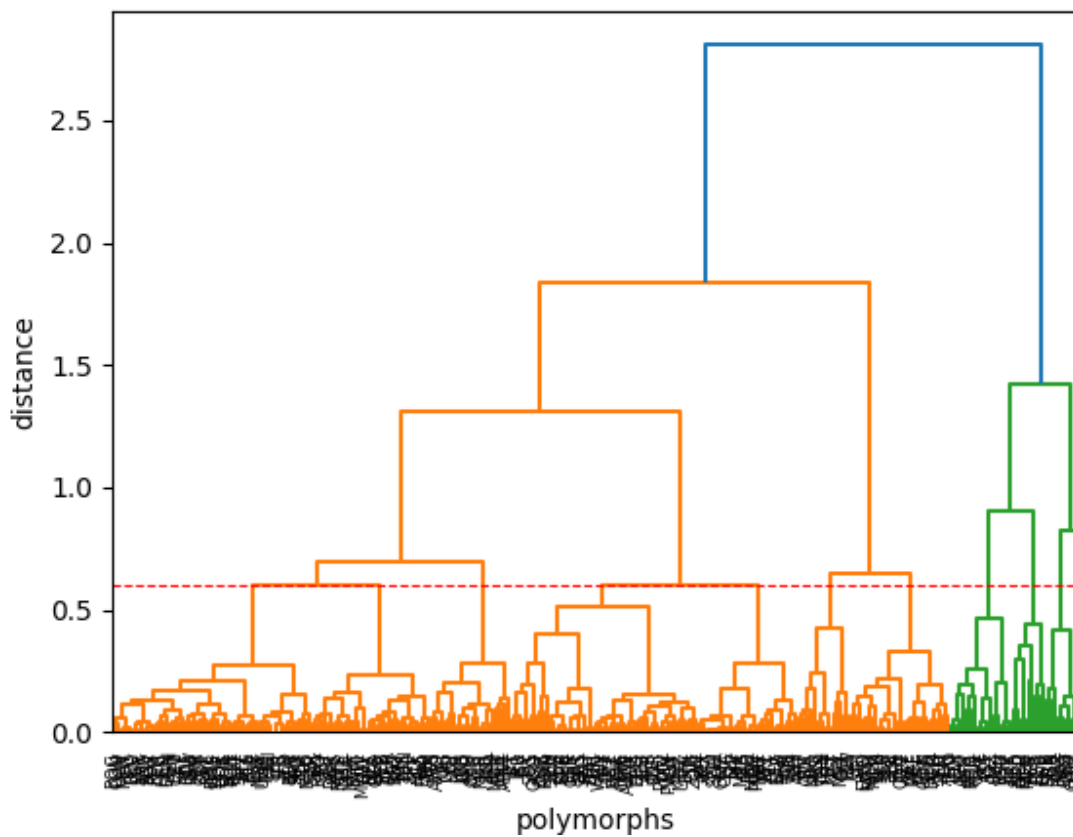


Figure S1: Dendrogram showing the horizontal distance of 0.59 below which a subgroup of 10 clusters are selected

Hyperparameters in training NNP (PANNA)

Table S1: Hyperparameters used in NNP training using PANNA package. Note that N_s is the number of symmetric function and N_θ the number of θ_s centres, N_a is the number of atomic species, R_c , cut-off radius, R_s , gaussian centre, η , gaussian width, and ζ , angular resolution parameter.

Parameter	Radial component	Angular component
$R_c(\text{\AA})$	6.5	4.2
$\eta(\text{\AA}^{-2})$	8.5	1.7
N_s	24	4
N_θ	-	8
ζ	50	50
$R_s(\text{\AA})$	0.5	0.5

- The hyperparameters in Table S1 leads to a G-vector of size given by $\frac{1}{2} (N_a(N_a + 1)) \times N_s \times N_\theta + N_a \times N_s(\text{radial}) = 3 \times 4 \times 8 + 2 \times 24 = 144$ per atom.
- The 20:20:1 architecture was used for the data accumulation stage of active learning cycle. This corresponds to $(144 \times 20 + 20) + (20 \times 20 + 20) + (20 \times 1 + 1) = 3341$ parameters per specie at a training step size of 200000. Data split used is 90 % and 10 % for training and validation.
- The 128:32:1 architecture was used after convergence of active learning cycle. This gives $(144 \times 128 + 128) + (128 \times 32 + 32) + (32 \times 1 + 1) = 22,721$ parameters per specie at a training step size of 600000. This improved the accuracy of the NNP model. Data split used is 90%, 5% and 5% for training, test and validation.

Allegro Hyperparameters

All parameters used the default setting in Allegro, except the following: Used a trainable besse function with radial cutoff of 6.0\AA and a spherical harmonics embedding of 2. Four hidden layers of dimension [64, 128, 256, 512] with nonlinear Sigmoid Linear Unit (Silu) activation for the 2-body embedding multilayer perceptron (MLP). Three hidden layers [512, 512, 512] with Silu non-linear activation function for latent MLP. Just one layer of dimension [64] was used for the final edge MLP. Dataset split of 90-10% was used for training and validation, using peratommseloss joint loss function for both energies and forces, and respective weights of 5 and 1. Used Adam¹ Optimizer with the following parameters $\beta_1=0.9$, $\beta_2=0.999$, and $\epsilon=10^{-8}$. The starting learning rate of 0.001 was used; resulting in a maximum epoch of 2441, at which point the learning rate dropped to 10^{-6} .

Table S2: Comparison between NNP and Allegro computational runtime for CHA zeolite (108 atoms per unit cell on Quevedo HPC. (T=Time correlation error = runtime \times train rmse, L_t =Looptime, N=no. of openMP and M=no. of MPI task)

Model	N	M	L_t (s)	t_{rmse} (meV/atom)	T (s meV/atom)
NNP(PANNA)	32	1	3061.22	3.00	9.184
Allegro	32	1	11088.6	3.50	39.032

Table S3: RMSEs of PANNA and Allegro Models.

model	Training		Validation	
	F(meV/ \AA)	E(meV/atom)	F(meV/ \AA)	E(meV/atom)
NNP	43.8	3.00	45.3	3.00
Allegro	3.92	3.52	9.13	4.39

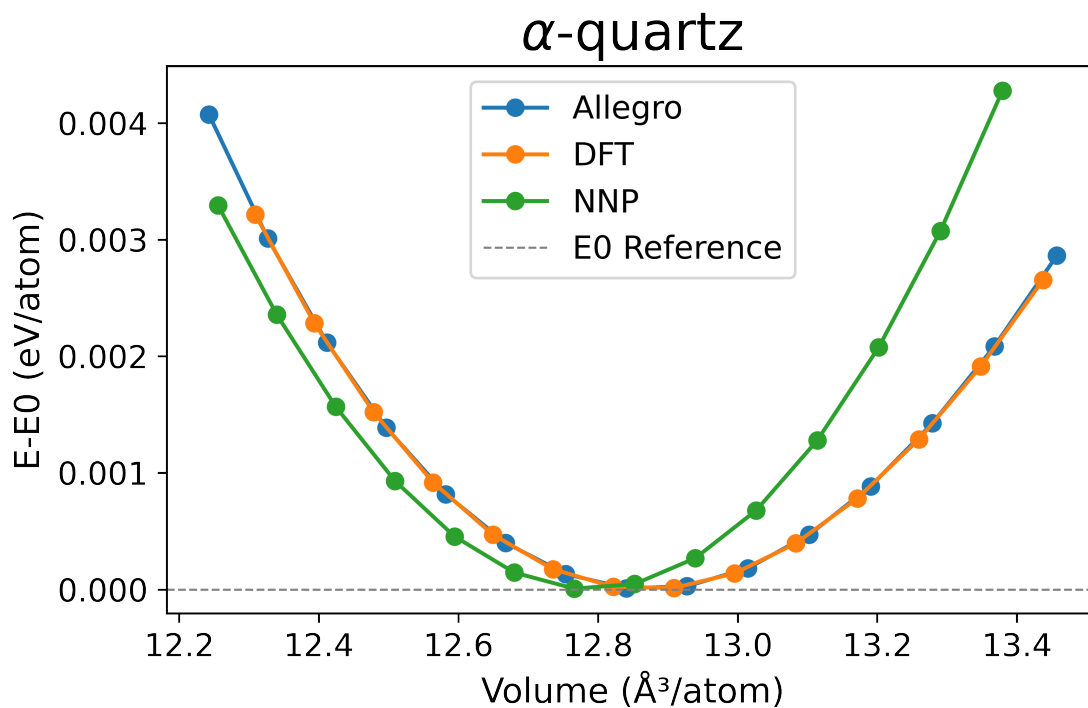


Figure S2: Energy(E) vs Volume (V) of α -quartz obtained by fitting energies to the Birch–Murnaghan equation of state. For each method, E_0 is the reference energy; i.e the energy of the unstrained polymorph.

Table S4: Table showing the lattice parameters of CHA, GIS, HEU and TON pure silica zeolites calculated using different MLIPs along side their corresponding DFT values. Note Nequip and DFT1 are from the previous work,² DeepMD and DFT2, from³ and NNP (PANNA), Allegro and DFT3, refers to the present work. Percent volume change is with respect to each methods referenced DFT.

Framework	method	a(Å)	b(Å)	c(Å)	α (deg)	β (deg)	γ (deg)	V(Å ³)	$\Delta V/V$ (%)
CHA	Nequip	9.285	9.285	9.285	93.87	93.87	93.87	795	0.13
	DFT1	9.286	9.286	9.286	94.06	94.06	94.06	794	
	DeepMD	9.335	9.335	9.335	94.218	94.218	94.218	806	0.75
	DFT3	9.325	9.325	9.325	94.218	94.218	94.21	804	
	PANNA	9.326	9.326	9.326	94.218	94.218	94.218	804	0.00
	Allegro	9.319	9.319	9.319	94.218	94.218	94.218	802	-0.25
	DFT3	9.325	9.325	9.325	94.218	94.218	94.218	804	
GIS	Nequip	9.539	9.539	9.886	90.00	90.00	90.00	900	-0.51
	DFT1	9.570	9.570	9.872	90.00	90.00	90.00	904	
	DeepMD	9.84	9.84	10.19	90.00	90.00	90.00	987	0.30
	DFT2	9.85	9.85	10.15	90.00	90.00	90.00	984	
	PANNA	10.131	10.131	9.794	90.00	90.00	90.00	1005	3.18
	Allegro	9.671	9.671	10.312	90.00	90.00	90.00	964	-0.10
	DFT3	9.740	9.740	10.264	90.00	90.00	90.00	974	
HEU	Nequip	17.346	17.466	7.326	90.00	116.10	90.00	1993	0.81
	DFT1	17.246	17.550	7.310	90.00	116.68	90.00	1977	
	DeepMD	17.56	17.64	7.41	90.00	116.10	90.00	2061	0.49
	DFT2	17.52	17.68	7.39	90.00	116.38	90.00	2051	
	PANNA	17.638	17.760	7.408	90.00	116.104	90.00	2072	0.78
	Allegro	17.586	17.708	7.405	90.00	116.104	90.00	2068	0.58
	DFT3	17.535	17.687	7.401	90.00	116.48	90.00	2056	
TON	Nequip	13.536	17.122	5.044	90.00	90.00	90.00	1169	-1.32
	DFT1	14.012	17.114	4.940	90.00	90.00	90.00	1185	
	DeepMD	14.02	17.3	10.07	90.00	90.00	90.00	2442	-7.78
	DFT2	14.07	17.87	10.53	90.00	90.00	90.00	2648	
	PANNA	14.318	17.708	5.305	90.00	90.00	90.00	1345	0.11
	Allegro	13.780	17.359	4.879	90.00	90.00	90.00	1167	-12.26
	DFT3	14.037	17.550	5.397	90.00	90.00	90.00	1330	

Table S5: Bulk modulus and elastic constants of α -cristobalite and α -quartz computed using NNP(PANNA), Allegro, and DFT

α -cristobalite				
method	K(Gpa)	C_{11} (Gpa)	C_{33} (Gpa)	C_{13} (Gpa)
exp. ⁴	15.95	63.2	42.4	-4.4
PANNA	40.24	55.09	74.42	13.37
Allegro	19.3	40.31	49.60	0.42
DFT	18.65	65.2	47.1	-4.1
α -quartz				
method	K(Gpa)	C_{11} (Gpa)	C_{33} (Gpa)	C_{13} (Gpa)
exp. ⁴	38.98	97.16	109.19	13.02
PANNA	58.34	109.00	149.84	35.78
Allegro	37.14	90.58	105.03	13.14
DFT	33.63	70.7	102.90	14.2

Phonon Dispersion at Gamma point for LTA zeolite

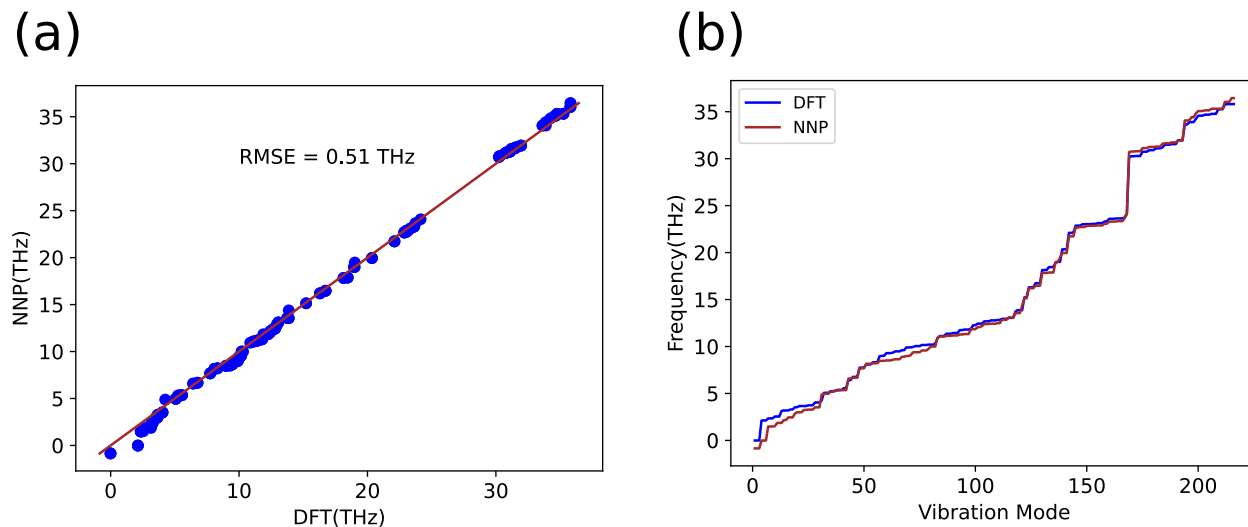


Figure S3: (a) Parity plot between the NNP-computed and DFT phonon frequencies at Gamma point of LTA zeolite. (b) Frequency versus phonon modes of vibrations at Gamma point computed using NNP and DFT of LTA zeolite.

Test of Model Transferability

Table S6: Success rate of NNP in predicting the energies of in-sample and out-of-sample polymorphs within energy thresholds of 3meV/atom and 25meV/atom for relaxed and unrelaxed structures.

unrelaxed		
Polymorphs	3meV/atom	25meV/atom
in-sample	100%	100%
out-of-sample	17%	78%
relaxed		
in-sample	80%	80%
out-of-sample	16%	84%

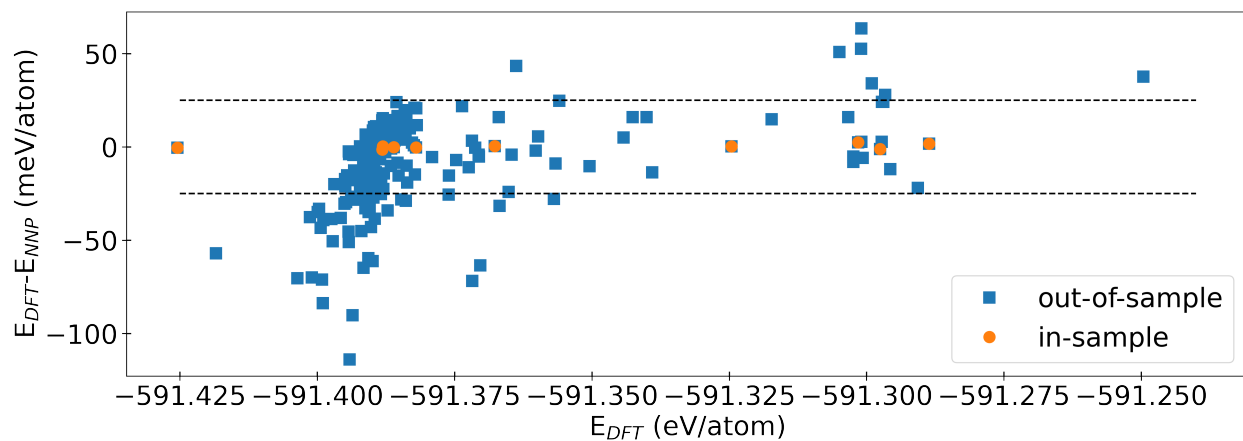


Figure S4: Errors in both in-sample and out-of-sample polymorphs relative to DFT energies on unrelaxed structures. The two horizontal lines are the ± 25 meV/atom bound.

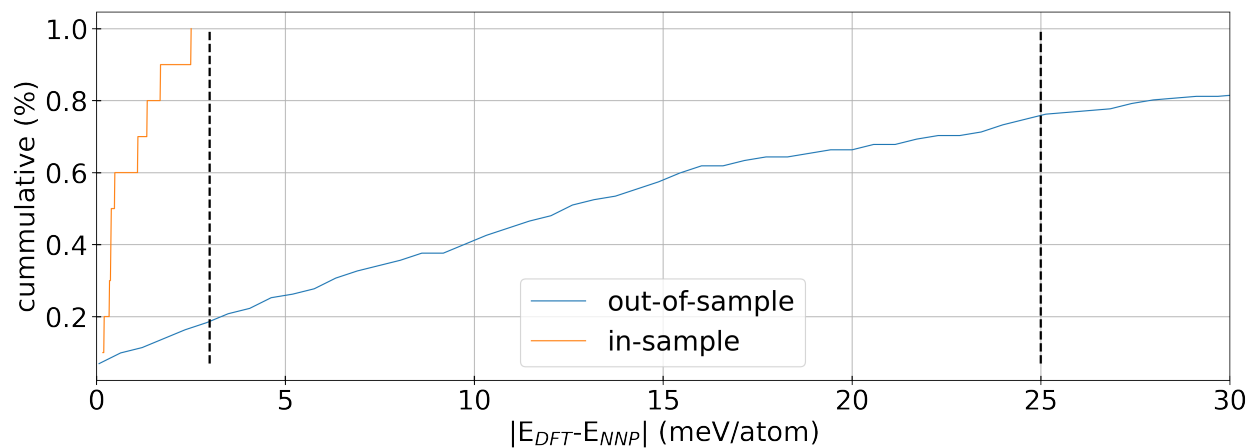


Figure S5: plot of Success rate relative to the errors on the energies of unrelaxed structures for both in-sample and out-of-sample polymorphs on unrelaxed. The black lines are the 3meV/atom and 25meV/atom threshold

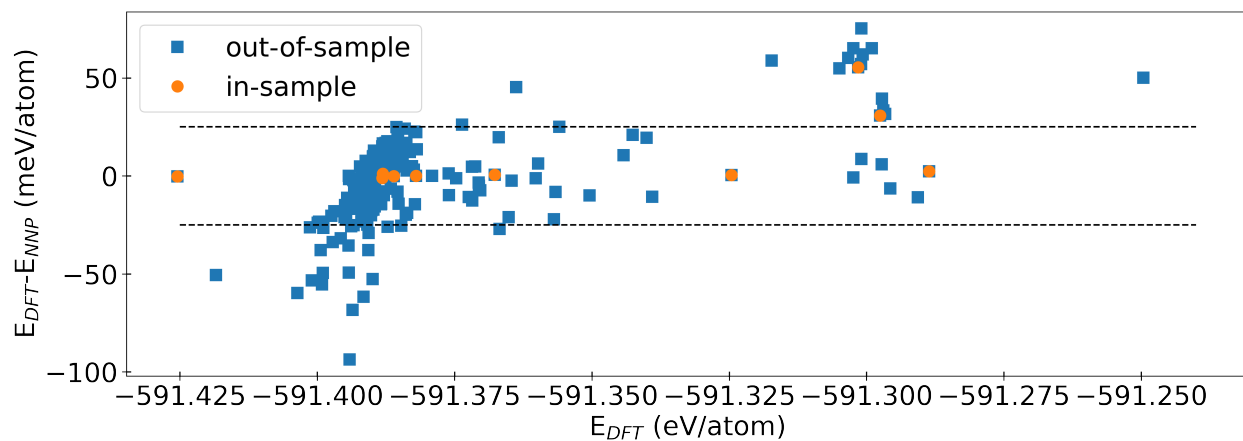


Figure S6: Errors in both in-sample and out-of-sample polymorphs relative to DFT energies on relaxed structures. The two horizontal lines are the ± 25 meV/atom bound.

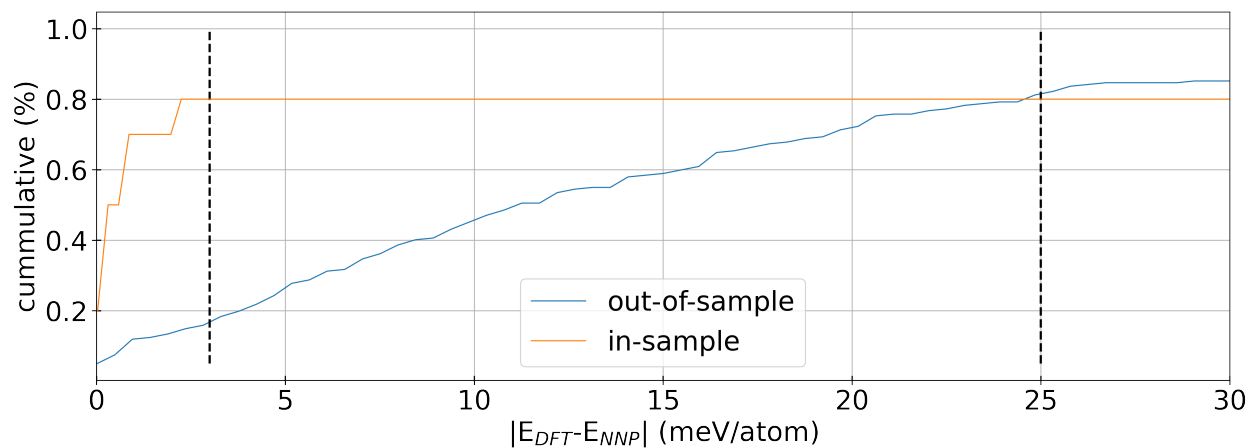


Figure S7: plot of Success rate relative to the errors on the energies of relaxed structures for both in-sample and out-of-sample polymorphs on relaxed. The black vertical lines are the 3meV/atom and 25meV/atom thresholds.

References

- (1) Kingma, D. P. Adam: A method for stochastic optimization. *arXiv preprint arXiv:1412.6980* **2014**,
- (2) Brugnoli, L.; Ducamp, M.; Coudert, F.-X. Neural network-based interatomic potential for the study of thermal and mechanical properties of siliceous zeolites. *The Journal of Physical Chemistry C* **2024**, *128*, 20512–20522.
- (3) Sours, T. G.; Kulkarni, A. R. Predicting structural properties of pure silica zeolites using deep neural network potentials. *The Journal of Physical Chemistry C* **2023**, *127*, 1455–1463.
- (4) Astala, R.; Auerbach, S. M.; Monson, P. Density functional theory study of silica zeolite structures: Stabilities and mechanical properties of SOD, LTA, CHA, MOR, and MFI. *The Journal of Physical Chemistry B* **2004**, *108*, 9208–9215.